Photothermal excitation of microcantilevers in liquid: effect of the excitation laser position on temperature and vibrational amplitude

Benjamin Andreas Bircher[1], Luc Duempelmann[1], Hans Peter Lang[2], Christoph Gerber[2], Thomas Braun[1]

[1]*Center for Cellular Imaging and NanoAnalytics, Biozentrum, University of Basel, Mattenstrasse 26, Basel CH-4058, Switzerland*
[2]*Swiss Nanoscience Institute, University of Basel, Klingelbergstrasse 82, Basel CH-4056, Switzerland*
E-mail: thomas.braun@unibas.ch

Published in Micro & Nano Letters; Received on 30th May 2013; Accepted on 1st August 2013

Demands to improve the sensitivity and measurement speed of dynamic scanning force microscopy and cantilever sensing applications necessitate the development of smaller cantilever sensors. As a result, methods to directly drive cantilevers, such as photothermal or magnetic excitation, are gaining in importance. Presented is a report on the effect of photothermal excitation of microcantilevers on the increase in steady-state temperature and the dynamics of higher mode vibrations. First, the local temperature increase upon continuous irradiation with laser light at different positions along the cantilever was measured and compared with finite element analysis data. The temperature increase was highest when the heating laser was positioned at the free end of the cantilever. Next, the laser intensity was modulated to drive higher flexural modes to resonance. The dependence of the cantilever dynamics on the excitation laser position was assessed and was in good agreement with the analytical expressions. An optimal position to simultaneously excite all flexural modes of vibration with negligible heating was found at the clamped end of the cantilever. The reports findings are essential for optimisation of the excitation efficiency to minimise the rise in temperature and avoid damaging delicate samples or functionalisation layers.

1. Introduction: Driving a microcantilever in air or liquid is a prerequisite for dynamic mode scanning force microscopy [1] and mechanical sensing applications [2]. Available techniques include acoustic, magnetic and photothermal excitation. Owing to its simplicity and robustness, acoustic excitation, which employs a vibrating piezoelectric crystal, is by far the most often applied. Its major drawbacks are spurious resonances, which result in the well-known 'forest of peaks' [3]. Particularly in liquid, the indirect energy transfer excites resonances originating from the chip body and fluid cell surfaces, impeding detection of the cantilever response. Although technical improvements have reduced some of these problems [4, 5], approaches in which the cantilever is directly excited are still preferred [6], particularly when the latter is immersed in viscous fluids. Magnetic excitation, where a magnetic field exerts a periodic force on the cantilever, has been successfully applied to drive cantilevers in liquid (for details see Han *et al.* [7]). When photothermal excitation is employed, an intensity-modulated laser periodically heats the cantilever and thus induces bending. This type of excitation was first applied to bridge resonators [8] and subsequently to cantilevers in air and liquids [9, 10]. The direct energy transfer avoids spurious resonances, and thus renders photothermal excitation suitable for atomic force microscopy [11, 12], force spectroscopy [13] and sensing applications [14]. Driving frequencies up to several megahertz have been accessed [15]. Furthermore, theoretical frameworks have identified the underlying mechanisms, allowing the experimental parameters to be optimised [16–18]. Highly efficient excitation can be achieved by using an asymmetric cantilever cross-section [19] and optimising the cantilever absorption properties to match the wavelength of the excitation laser [15]. Understanding laser-induced heating of the cantilever and its surroundings is of major importance because it could, for example, alter the surrounding fluid properties [20] or damage delicate samples.

Here, we report the influence of the excitation laser position on the local steady-state temperature distribution and the amplitude of higher flexural modes of vibration in liquid. Steady-state heating by an incident laser with constant intensity is modelled using finite element analysis and compared with the temperature indirectly measured via bi-material bending of the gold-coated cantilever [21]. By focusing the intensity-modulated excitation laser at different positions along the cantilever, the amplitudes of higher flexural modes of vibration are measured and compared with the analytical expressions [16, 22].

2. Materials and methods

2.1. Experimental setup: Fig. 1 shows the experimental setup consisting of two laser diodes to, respectively, heat (LD_{EX}, 406 nm) and detect the deflection (LD_{DE}, 780 nm) of the cantilever. The wavelengths are chosen so that ~67% of the

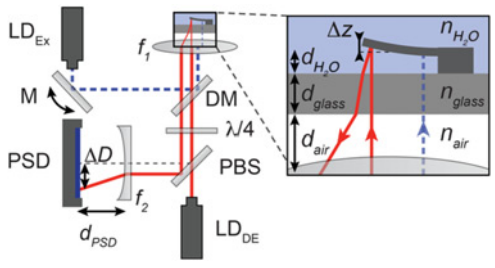

Figure 1 *Setup employed to heat cantilever and detect its deflection*
Detection beam (red line) originating from 780 nm laser diode (LD_{DE}) is focused onto cantilever using 4× objective (f_1)
Reflected beam directed onto position sensitive detector (PSD) using polarising beam splitter
Concave lens (f_2) that is separated from PSD by d_{PSD} is inserted to enhance deflection signal
Δz and ΔD are deflection of cantilever and induced laser spot displacement on PSD, respectively
Heating/driving laser (LD_{EX}, 406 nm; blue dashed line) is coupled in using dichroic mirror
Mirror (M) allows its position on cantilever to be controlled
Distances are cantilever-glass slide spacing d_{H_2O}, thickness of the glass slide d_{glass} and glass slide-objective (f_1) distance d_{air}
Parameters n_{H_2O}, n_{glass} and n_{air} are refractive indices of corresponding media

doi: 10.1049/mnl.2013.0352

heating and < 3% of the detection laser intensity is absorbed by the cantilever gold coating. The detection laser spot is positioned at the tip of the cantilever during all experiments, resulting in the highest response for all the flexural modes of vibration. The Gaussian spot size on the cantilever, determined using the knife-edge method [23], was 12 μm for LD_{DE} and 29 μm for LD_{EX}. The deflection of the cantilever Δz is geometrically related to the displacement ΔD of the laser spot on the position sensitive detector (PSD) [24]. Considering the different refractive indices of the media the laser beam passes through (see (1))

$$\Delta z = \frac{L}{4} \frac{|f_2|}{n_{H_2O}\left(\frac{d_{H_2O}}{n_{H_2O}} + \frac{d_{glass}}{n_{glass}} + \frac{d_{air}}{n_{air}}\right)\left(|f_2| + d_{PSD}\right)} \Delta D \tag{1}$$

The parameters are: focal length of the concave lens, $f_2 = -50$ mm; length of the cantilever, $L = 500$ μm; refractive indices, $n_{H_2O} = 1.33$, $n_{glass} = 1.50$, $n_{air} = 1.00$; distances, $d_{H_2O} = 0.5$ mm, $d_{glass} = 1.0$ mm, $d_{air} = 43.5$ mm and $d_{PSD} = 95$ mm as indicated in Fig. 1. The static displacement on the PSD is 10× amplified (AM502, Tektronix; bandwidth: 100 Hz) and recorded using a custom LabVIEW (National Instruments) software. For dynamic measurements, an AC signal is modulated on the DC component of the excitation laser. The cantilever response is 10× amplified (SIM911, Stanford Research Systems; bandwidth: 1 MHz) and recorded using a vector network analyser (MS4630B, Anritsu). Silicon cantilevers with nominal dimensions of $500 \times 100 \times 4$ μm^3 (IBM Zurich Research Laboratory, Rüschlikon, Switzerland) were used for the experiments. Their bottom surface is coated with a 20 nm-thick gold layer. More details of the setup and the cantilever preparation are provided in [25]. The cantilevers were immersed and kept in nanopure water for all experiments. The temperature of the fluid cell was stabilised at 293.15 K to an accuracy of 0.3 K.

2.2. Steady-state temperature increase by continuous laser irradiation

2.2.1 Temperature measured by bi-material cantilever deflection: The difference in the linear thermal expansion coefficients of the two materials causes a bi-material cantilever beam, subjected to a temperature change of ΔT, to deflect by Δz. Thus, deflection can be used as a measure of the average cantilever temperature, assuming a homogeneous temperature distribution along the beam. Even though the response is complex and nonlinear over a wide temperature range [26], it can be linearised for small temperature changes [21, 27]

$$\Delta T = \frac{t_{Si}^2 K\left(t_{Au},\ t_{Si},\ E_{Si},\ E_{Au}\right)}{3L^2\left(\gamma_{Au} - \gamma_{Si}\right)\left(t_{Au} + t_{Si}\right)} \Delta z \tag{2}$$

The thickness of the cantilever t_{Si} was determined in a calibration step (see Section 4) and the thickness of the deposited gold layer t_{Au} was 20 nm. K is a function depending on the thicknesses and Young's moduli of the two layers and is provided in [21]. The linear thermal expansion coefficients and Young's moduli were $\gamma_{Si} = 2.59 \times 10^{-6}$ K^{-1}, $\gamma_{Au} = 14.2 \times 10^{-6}$ K^{-1}, $E_{Si} = 169$ GPa and $E_{Au} = 79$ GPa [26]. The deflection Δz was measured while positioning the laser at different places on the cantilever and switching on the laser until a steady-state deflection was reached. To account for small variations in the baseline (< 5 nm), the deflection before laser switch-on was subtracted from the steady-state deflection after laser switch-on. Two different incident laser powers were employed for these measurements: 2.4 and 4.9 mW with corresponding power densities of 2.3 and 4.6 MW/m^2, respectively, on the cantilever.

2.2.2 Temperature simulated by finite element (FE) analysis: FE simulations reported in the literature were performed to study the effect of laser irradiation on the microstructures [18, 28–30]. In the present work, the increase in temperature of the cantilever immersed in water, because of the heat deposited by the incident excitation laser, was simulated via a three-dimensional FE analysis using the Heat Transfer module in COMSOL Multiphysics [31]. Owing to the small scale and localisation of the heat sources, conductive heat transfer was assumed to be the major dissipative mechanism, and convective heat transfer and radiation were assumed to be negligible. The heat equation [31] then reduces to

$$\rho C_p \frac{\partial T}{\partial t} - \nabla(k \nabla T) = Q \tag{3}$$

where ρ, C_p, k, Q and T are the mass density, the heat capacity at constant pressure, the thermal conductivity, an inward heat flux and the temperature. All material properties were taken from the COMSOL Multiphysics material library. A total of ~300 000 elements were meshed; thereby, the region around the cantilever was meshed with higher resolution. More than 97% of the detection laser power was reflected. Therefore, it does not cause significant heating, and was not considered in the simulations. The excitation laser was modelled as a boundary heat source on the surface of the cantilever, thus neglecting light absorption by the surrounding fluid. Since the penetration depth of the optical field is very small compared with the thickness of the cantilever, the absorbed power density was estimated to be $Q_{EX} = P_{in}(1 - R)/(\pi r^2)$, where P_{in} is the incident laser power, $R = 0.33$ the reflectance at wavelength $\lambda = 406$ nm and $r = 15$ μm is the radius of the heat source. The boundary conditions were defined as follows: the silicone cell enclosing the fluid was assumed to be thermally insulating; the bottom face of the fluid and the cantilever chip (see Fig. 1) were taken to be in ideal thermal contact with the glass slide. The vertical faces of the glass slide were set as open boundaries, thus extending it infinitely in the horizontal direction and allowing heat to flow outwards; being temperature controlled, the bottom of the glass slide was modelled as a heatsink at a constant temperature of 293.15 K. Numerical results were processed by taking cross-sectional temperature profiles and calculating the average temperature of the cantilever.

2.3. Photothermal excitation of higher flexural modes:

Photothermal excitation is achieved by an intensity-modulated laser, which periodically heats the microcantilever and, thus, induces vibration. The force per length exerted on the cantilever through the differential longitudinal stress produced by the heat from the laser, is a convolution between the temperature distribution ΔT and the second derivative of the spatial mode profile ϕ_n of the vibrating cantilever [16, 22]. Under the assumption of harmonic vibration, the normalised amplitude of vibration at the tip of the cantilever scales linearly with the applied force per unit length, leading to the following expression

$$A(x_0) = A_0 \int_0^L \Delta T(x; x_0) \frac{d^2 \phi_n(x)}{dx^2} dx \tag{4}$$

where x is the coordinate along the cantilever axis and x_0 the position of the excitation laser; A_0 is a normalisation factor determined for each mode individually; $\phi_n(x)$ is the spatial distribution of the nth eigenmode of the cantilever [32]; $\Delta T(x; x_0)$ is the temperature distribution along the beam. For dynamic cantilever excitation, only the alternating component of $\Delta T(x; x_0)$ is of importance. Therefore ΔT was described by a Gaussian function resembling the intensity distribution of the laser spot. To obtain the amplitude, resonance spectra were recorded while moving the excitation laser along the cantilever. Fitting a simple

harmonic oscillator model allowed the angular deflection amplitude to be determined for each mode individually. To precisely determine the relative excitation spot position and normalise the data, (4) was fitted to the profiles of modes 2–6 simultaneously using a global fit algorithm. For all dynamic experiments, a peak-to-peak amplitude of 7 mW was modulated onto a constant laser power of 4.9 mW.

3. Results and discussion

3.1. Steady-state temperature upon continuous laser irradiation in liquid: The steady-state temperature increase in liquid, induced by continuous laser irradiation at different positions along the cantilever, was evaluated by two independent approaches: (i) indirect measurement by the bi-material bending of the cantilever and (ii) FE simulations.

First, the thickness of the bi-material cantilever was calibrated. The ambient temperature was changed stepwise from 293.15 to 297.15 K, resulting in upward cantilever deflections ranging from 0 to 36 nm. As reported previously, [27], and discussed above (see Section 2), the temperature-deflection dependence was linear (correlation coefficient $R = 0.998$). By fitting (2) to the data, the thickness of the cantilever was determined to be $t_{Si} = 3.0$ µm. The calibrated thickness deviates from the nominal value (4 µm) because of variations in the fabrication process and systematic deviations in the geometrically determined deflection (1). After calibration, the deflection upon continuous laser irradiation at different positions along the beam (illustrated in Fig. 2*a*) was recorded and converted into an average increase in temperature using (2) (Fig. 2*b*). Close to the chip, a thicker support region defines the clamped end of the cantilever [position (1), Fig. 2*a*]. Positioning the laser further towards the tip of the cantilever [positions (2) and (3), Fig. 2*a*], resulted in higher deflections and, thus, higher temperatures as shown in Fig. 2*b*. Turning on the laser was followed by heating-related deflection resulting in a steady-state value within a few seconds; turning the laser off again reversed the process. The maximum deflection was 56 nm, indicating an increase in the average cantilever temperature of about 6 K. The observed reversibility and repeatability of this process indicates that ablation of the cantilever coating, previously observed at higher power densities in air [29], did not occur.

The results of the FE simulations employed to determine the temperature profiles of the cantilever and its surroundings are shown in Fig. 3*a*. A confined hot spot forms around the position of the heating laser. The maximal local temperature change found by FE analysis was 11 K for 4.9 mW laser irradiation at the tip of the cantilever. The average increase in the temperature of the cantilever material was calculated from the simulated data (solid lines in Fig. 3*b*), for comparison with the values derived from the measured deflection of the cantilever using (2) (markers in Fig. 3*b*). As indicated by the simulations, the assumed homogeneous temperature distribution is a poor description of the temperature profile along the beam (Fig. 3*a*). This accompanying uncertainty in the experimentally derived temperature data may be the main reason why the simulation apparently overestimates the average temperature increase in the first half of the cantilever and underestimates it towards the tip. More importantly, even though the two independent datasets differ slightly, both reveal the same temperature behaviour along the cantilever beam (Fig. 3*b*). The shape of the profiles identifies thermal conduction through the cantilever material as the major mechanism for heat dissipation. Moving the heating laser closer to the clamped end (support) improves the thermal conductance [33], dissipating a larger fraction of the incident power through the cantilever chip. Owing to its lower thermal conductivity, the surrounding liquid provides insufficient heat drain when the laser is positioned towards the tip of the cantilever, resulting in a larger temperature increase.

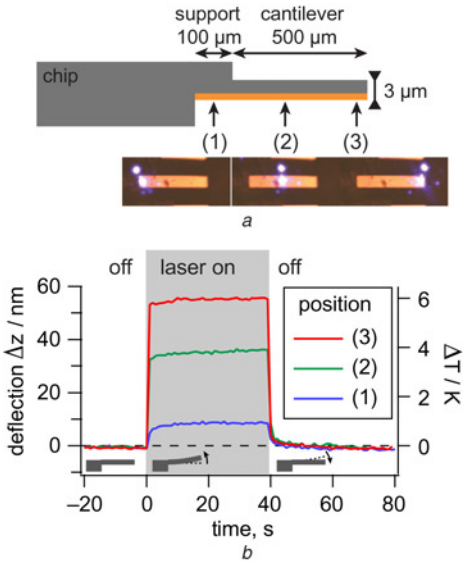

Figure 2 *Static deflection induced by laser heating*
a Schematic of sensor indicating 20 nm gold layer (yellow) and thicker support region (length 100 µm), which connects the cantilever (500 µm) to the chip (drawing not in scale)
Laser spot positioned on support (1), towards middle of cantilever (2) and at its tip (3) as shown by micrographs; second spot (beside cantilever) is reflection from glass slide
b Cantilever deflection Δz and increase in average cantilever temperature ΔT upon 4.9 mW laser irradiation at different positions on cantilever

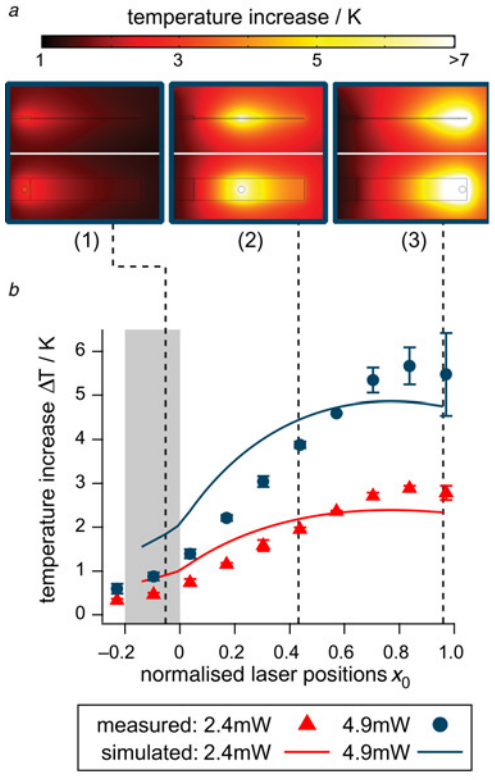

Figure 3 *Steady-state temperatures for different laser positions x_0*
a Side and top views of simulated profiles along central cross-section of cantilever for laser positions (power 4.9 mW) indicated by numbers in Fig. 2*a*
b Simulated and measured average temperatures of cantilever upon laser irradiation with powers of 2.4 and 4.9 mW
Temperature determined from deflection of bi-material cantilever (shown are the mean and standard deviation of three consecutive measurements)
Shaded area indicates thicker cantilever support region (Fig. 2*a*)

doi: 10.1049/mnl.2013.0352

3.2. Dependence of laser spot position on higher mode excitation: The dynamic response of higher flexural modes of vibration excited by an intensity-modulated laser at different positions along a cantilever immersed in liquid was investigated. A photothermally driven amplitude spectrum is shown in Fig. 4*a*. The cantilever resonance peaks are well resolved because the spectrum is free of spurious resonances. The fundamental mode is not recorded, because its resonance frequency is below the highpass filter frequency of the excitation electronics. Fig. 4*b* shows the normalised amplitude for flexural modes of vibration 2–6 for different excitation laser positions. Except for the region towards the clamped end of the cantilever ($x_0 = 0$), the amplitude profiles are in good agreement with the theoretical values (4). An optimal excitation position within the support region ($x_0 = -0.06$) was identified for mode 3 and higher (Fig. 4, black arrow). It resulted in amplitudes up to 2.5 times higher than those obtained by positioning the laser on the cantilever itself and the difference was more pronounced for higher modes. This feature is most probably because of the specific geometry of the cantilevers employed: the thicker support region [position (1) in Fig. 2*a*] is an efficient heatsink. Therefore, the temperature decreases more rapidly after a laser pulse, allowing higher local peak-to-peak temperature variations at high frequencies. These are in turn transduced into larger vibrational amplitudes and, thus, a more efficient excitation of higher modes, or higher frequencies in general.

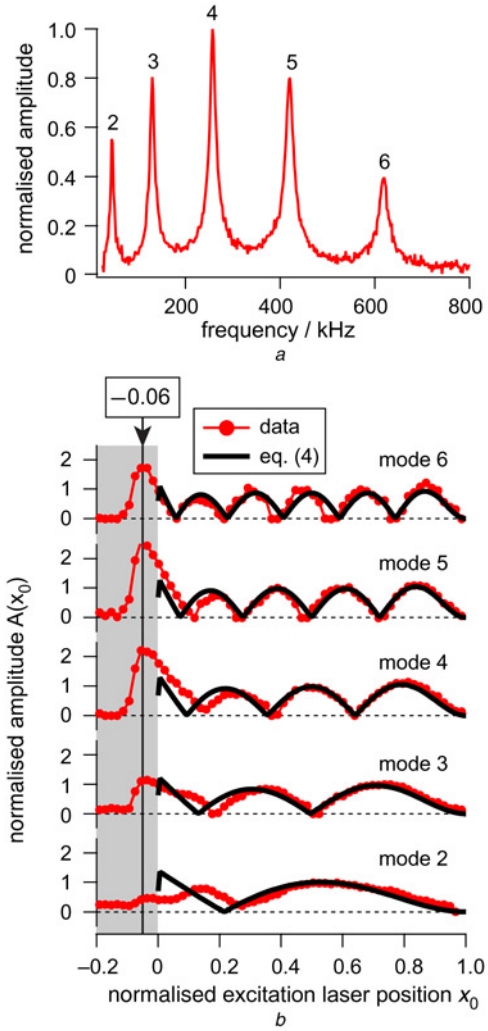

Figure 4 *Normalised amplitude spectrum recorded with excitation laser at optimal position (Fig. 4a) (position −0.06; black arrow in panel of Fig. 4b); flexural mode numbers are indicated and amplitude is normalised to the highest peak. Amplitudes of flexural modes 2–6 against excitation laser position x_0 on cantilever (Fig. 4b); red markers indicate measured values and solid black lines denote theoretical values; shaded area indicates support region (Fig. 2a); profiles normalised to theoretical values of each mode separately*

4. Conclusions: Understanding the interaction of laser radiation with microstructures is of major importance for the optical excitation of microcantilevers in fluid, picowatt calorimetry [33], thermodynamic measurements of thin films [29] and the dynamics of microactuators [28]. FE simulations and deflection-derived measurements of the laser-induced temperature increase at different positions on a microcantilever were in good agreement. Conductive heat transfer through the cantilever material was identified as the dominant heat dissipation mechanism of a cantilever in liquid irradiated by a laser. Furthermore, the dynamic response of the cantilever, driven photothermally by an intensity-modulated laser at different positions, was studied. These findings allowed the optimal position of the excitation laser spot on the cantilever to be determined for different flexural modes of vibration. Placing the spot in the support region of the cantilever used, resulted in the most efficient excitation along all flexural modes greater than two, whereas the temperature increase was minimal (<2 K). We hypothesise that the efficient heatsink properties of the support promote local high-frequency temperature variations, which would explain why the effect was more pronounced at higher frequencies. These findings are of particular interest because high resonance frequencies, achieved by using higher modes or smaller cantilever dimensions, increase the sensitivity [2].

Improving the excitation efficiency and thus reducing the temperature increase, allows optical excitation to be employed without damaging functionalisation layers in sensing applications or sample surfaces in dynamic mode scanning force microscopy by thermal denaturation. The major parameters to be considered are: (i) the cantilever geometry and material, (ii) the excitation laser spot size determining the power density and (iii) the position of the excitation laser on the cantilever.

5. Acknowledgments: The authors acknowledge H. Stahlberg (C-CINA, University of Basel, Switzerland) for providing infrastructure and facilities; S.A. Müller (C-CINA) for critically reading the manuscript; M. Despont and U. Drechsler (IBM Research GmbH, Rueschlikon, Switzerland) for providing cantilever arrays; K.N. Goldie (C-CINA) for determining the cantilever dimensions by scanning electron microscopy. This work was supported by SNF grant 200021/130594, NCCR Nano and ARGOVIA project NoViDeMo.

6 References

[1] Jalili N., Laxminarayana K.: 'A review of atomic force microscopy imaging systems: application to molecular metrology and biological sciences', *Mechatronics*, 2004, **14**, (8), pp. 907–945

[2] Johnson B.N., Mutharasan R.: 'Biosensing using dynamic-mode cantilever sensors: a review', *Biosens. Bioelectron.*, 2012, **32**, (1), pp. 1–18

[3] Schäffer T.E., Cleveland J.P., Ohnesorge F., Walters D.A., Hansma P.K.: 'Studies of vibrating atomic force microscope cantilevers in liquid', *J. Appl. Phys.*, 1996, **80**, (7), pp. 3622–3627

[4] Maali A., Hurth C., Cohen-Bouhacina T., Couturier G., Aimé J.-P.: 'Improved acoustic excitation of atomic force microscope cantilevers in liquids', *Appl. Phys. Lett.*, 2006, **88**, (16), p. 163504

[5] Asakawa H., Fukuma T.: 'Spurious-free cantilever excitation in liquid by piezoactuator with flexure drive mechanism', *Rev. Sci. Instrum.*, 2009, **80**, (10), p. 103703

[6] Labuda A., Kobayashi K., Kiracofe D., Suzuki K., Gruetter P.H., Yamada H.: 'Comparison of photothermal and piezoacoustic excitation methods for frequency and phase modulation atomic force microscopy in liquid environments', *AIP Adv.*, 2011, **1**, (2), p. 022136

[7] Han W., Lindsay S.M., Jing T.: 'A magnetically driven oscillating probe microscope for operation in liquids', *Appl. Phys. Lett.*, 1996, **69**, (26), pp. 4111–4113
[8] Venkatesh S., Culshaw B.: 'Optically activated vibrations in a micromachined silica structure', *Electron. Lett.*, 1985, **21**, (8), p. 315–317
[9] Lammerink T.S.J., Elwenspoek M., Fluitman J.H.J.: 'Optical excitation of micro-mechanical resonators'. IEEE Micro Electro Mechanical Systems (MEMS 1991), Nara, Japan, 1991, pp. 160–165
[10] Inaba S., Akaishi K., Mori T., Hane K.: 'Analysis of the resonance characteristics of a cantilever vibrated photothermally in a liquid', *J. Appl. Phys.*, 1993, **73**, (6), pp. 2654–2658
[11] Ratcliff G.C., Erie D.A., Superfine R.: 'Photothermal modulation for oscillating mode atomic force microscopy in solution', *Appl. Phys. Lett.*, 1998, **72**, (15), pp. 1911–1913
[12] Labuda A., Kobayashi K., Miyahara Y., Grütter P.H.: 'Retrofitting an atomic force microscope with photothermal excitation for a clean cantilever response in low Q environments', *Rev. Sci. Instrum.*, 2012, **83**, (5), p. 053703
[13] Stahl S.W., Puchner E.M., Gaub H.E.: 'Photothermal cantilever actuation for fast single-molecule force spectroscopy', *Rev. Sci. Instrum.*, 2009, **80**, (7), p. 073702
[14] Ramos D., Mertens J., Calleja M., Tamayo J.: 'Photothermal self-excitation of nanomechanical resonators in liquids', *Appl. Phys. Lett.*, 2008, **92**, (17), p. 173108
[15] Nishida S., Kobayashi D., Kawakatsu H., Nishimori Y.: 'Photothermal excitation of a single-crystalline silicon cantilever for higher vibration modes in liquid', *J. Vac. Sci. Technol. B.*, 2009, **27**, (2), pp. 964–968
[16] Ramos D., Tamayo J., Mertens J., Calleja M.: 'Photothermal excitation of microcantilevers in liquids', *J. Appl. Phys.*, 2006, **99**, (12), p. 124904
[17] Wang S., Wang X., Liu Y., Huang B.: 'Parameter optimization of microcantilevers optically excited by a semiconductor laser with optical feedback', *Optik.*, 2009, **120**, (13), pp. 676–682
[18] Ilic B., Krylov S., Craighead H.G.: 'Theoretical and experimental investigation of optically driven nanoelectromechanical oscillators', *J. Appl. Phys.*, 2010, **107**, (3), p. 034311
[19] Kiracofe D., Kobayashi K., Labuda A., Raman A., Yamada H.: 'High efficiency laser photothermal excitation of microcantilever vibrations in air and liquids', *Rev. Sci. Instrum.*, 2011, **82**, (1), p. 013702
[20] Kim S., Kihm K.D.: 'Experimental verification of the temperature effects on Sader's model for multilayered cantilevers immersed in an aqueous medium', *Appl. Phys. Lett.*, 2006, **89**, (6), p. 061918
[21] Barnes J.R., Stephenson R.J., Woodburn C.N., *ET AL.*: 'A femtojoule calorimeter using micromechanical sensors', *Rev. Sci. Instrum.*, 1994, **65**, (12), pp. 3793–3798
[22] Vassalli M., Pini V., Tiribilli B.: 'Role of the driving laser position on atomic force microscopy cantilevers excited by photothermal and radiation pressure effects', *Appl. Phys. Lett.*, 2010, **97**, (14), p. 143105
[23] de Araújo M.A.C., Silva R., de Lima E., Pereira D.P., de Oliveira P.C.: 'Measurement of Gaussian laser beam radius using the knife-edge technique: improvement on data analysis', *Appl. Opt.*, 2009, **48**, (2), pp. 393–396
[24] Mishra R., Grange W., Hegner M.: 'Rapid and reliable calibration of laser beam deflection system for microcantilever-based sensor setups', *J. Sensors.*, 2012, **2012**, p. ID617386
[25] Bircher B.A., Duempelmann L., Renggli K., *ET AL.*: 'Real-time viscosity and mass density sensors requiring microliter sample volume based on nanomechanical resonators', *Anal. Chem.*, 2013, **85**, (18), pp. 8676–8683
[26] Ramos D., Mertens J., Calleja M., Tamayo J.: 'Study of the origin of bending induced by bimetallic effect on microcantilever', *Sensors*, 2007, **7**, (9), pp. 1757–1765
[27] Shen S., Narayanaswamy A., Goh S., Chen G.: 'Thermal conductance of bimaterial microcantilevers', *Appl. Phys. Lett.*, 2008, **92**, (6), p. 063509
[28] Liu C., Zhang D., Zhang H., Jiang J.Z.: 'Dynamic characteristics of micro-optothermal expansion and optothermal microactuators', *Micro Nano Lett.*, 2009, **4**, (1), pp. 9–15
[29] Burke B.G., LaVan D.A.: 'Laser heating and detection of bilayer microcantilevers for non-contact thermodynamic measurements', *Appl. Phys. Lett.*, 2013, **102**, (2), p. 021916
[30] Moulin A.M., Stephenson R.J., Welland M.E.: 'Micromechanical thermal sensors: comparison of experimental results and simulations', *J. Vac. Sci. Technol. B*, 1997, **15**, (3), pp. 590–596
[31] COMSOL Multiphysics – Modeling Guide, VERSION 3.5a. COMSOL, available at http://www.comsol.com; 2008
[32] Paolino P., Tiribilli B., Bellon L.: 'Direct measurement of spatial modes of a microcantilever from thermal noise', *J. Appl. Phys.*, 2009, **106**, (9), p. 094313
[33] Canetta C., Narayanaswamy A.: 'Sub-picowatt resolution calorimetry with a bi-material microcantilever sensor', *Appl. Phys. Lett.*, 2013, **102**, (10), p. 103112

doi: 10.1049/mnl.2013.0352